

MEASURING, MONITORING AND MODELING
CONCRETE PROPERTIES

Measuring, Monitoring and Modeling Concrete Properties

An International Symposium dedicated to
Professor Surendra P. Shah, Northwestern
University, U.S.A.

Edited by

MARIA S. KONSTA-GDOUTOS
Democritus University of Thrace, Xanthi, Greece

 Springer

A C.I.P. Catalogue record for this book is available from the Library of Congress.

ISBN-10 1-4020-5103-4 (HB)
ISBN-13 978-1-4020-5103-6 (HB)
ISBN-10 1-4020-5104-2 (e-book)
ISBN-13 978-1-4020-5104-3 (e-book)

Published by Springer,
P.O. Box 17, 3300 AA Dordrecht, The Netherlands.

www.springer.com

Cover picture

10 m x 10 m image of C-S-H Gel from triboindenter.
Courtesy of Ms. Paramita Mondal, Ph. D. student, Center for ACBM, Northwestern University

Printed on acid-free paper

All Rights Reserved

© 2006 Springer

No part of this work may be reproduced, stored in a retrieval system, or transmitted in any form or by any means, electronic, mechanical, photocopying, microfilming, recording or otherwise, without written permission from the Publisher, with the exception of any material supplied specifically for the purpose of being entered and executed on a computer system, for exclusive use by the purchaser of the work.

Printed in the Netherlands.

Contents

Preface of ECF16 Chairman Emmanuel E. Gdoutos.....	xiii
Editor's Preface.....	xv
Surendra P. Shah	xvii
Scientific Advisory Board.....	xix

Engineering Performance and Modeling for High-Performance Cementitious Composites

Effect of Fibre Distribution on the Fatigue Performance and Autogenous Shrinkage of CARDIFRC [®]	3
<i>D. Nicolaidis, A. Kanellopoulos and B.L. Karihaloo</i>	
Structural Applications of HPFRCC in Japan.....	17
<i>K. Rokugo, M. Kunieda and S. Miyazato</i>	
Simulation of the Tensile Stress-Strain Behavior of Strain Hardening Cementitious Composites.....	25
<i>J. Yang and G. Fischer</i>	
Effect of the Test Set-Up and Curing Conditions on Fracture Behavior of Strain Hardening Cement-Based Composites (SHCC)	33
<i>V. Mechtcherine and J. Schulze</i>	
Condition for Strain-Hardening in ECC Uniaxial Test Specimen	41
<i>L. Dick-Nielsen, H. Stang and P.N. Poulsen</i>	
Experimental and Numerical Analysis of UHPFRC Plates and Shells	49
<i>E.M.R. Fairbairn, R.D. Toledo Filho, R.C. Battista, J.H. Brandão, J.I. Rosa and S. Formagini</i>	
FRC and HPFRC Composites: From Constitutive Behaviour to Structural Applications	59
<i>M. di Prisco and M. Colombo</i>	
Tailored Composite UHPFRC-Concrete Structures.....	69
<i>E. Denarié and E. Brühwiler</i>	

Hybrid Fiber Reinforced Concrete.....	77
<i>L. Vandewalle</i>	
Preventing Autogenous Shrinkage of High-Performance Concrete Structures by Internal Curing	83
<i>D. Cusson and T. Hoogeveen</i>	
Thermo-Mechanical Analysis of Young Concrete: Application to a Restrained Slab...	91
<i>M. Azenha, R. Faria and J.A. Figueiras</i>	
Modeling High Strength Concrete using Finite Element with Embedded Cohesive Crack	99
<i>A.M.Fathy, J. Planas, J.M. Sancho, D.A. Cendón and J.C. Gálvez</i>	
Size Effect of Concrete: Uniaxial and Flexural Compression	107
<i>A.L. Gamino, J. U. A. Borges and T.N. Bittencourt</i>	
Embedded Crack Elements with Non-Uniform Discontinuity Modes	115
<i>O.L. Manzoli and P.B. Shing</i>	
Efficient Strengthening Technique for Reinforced Concrete Slabs	125
<i>E. Bonaldo, J.A.O. Barros and P.B. Lourenço</i>	
Bending Performance of High Strength Steel Fibre Reinforced Concrete: Static and Fatigue Loading Conditions	133
<i>E.S. Lappa, C.R. Braam and J.C. Walraven</i>	
Axial Symmetry Analyses of Punching Shear in Reinforced Flat Slabs	139
<i>L. Trautwein, T. Bittencourt, R. Faria, J.A. Figueiras and R. Gomes</i>	
Bond-Slip Behavior of Reinforcement in NSC and HSC with and without Steel Fibers.....	145
<i>A. Dancygier, A. Katz and U. Wexler</i>	
Application of Inverse Analysis to Shrinkage and Creep Models	151
<i>L.C. de Almeida, J.L.A. de Oliveira e. Sousa and J. de Azevedo Figueiras</i>	
<i>Fracture and Deformation of Cement Based Composites</i>	
Effects of Lightweight Aggregates on Autogenous Deformation in Concrete	163
<i>B. Akcay and M.A. Tasdemir</i>	
Fracture Behavior of High Performance Fiber Reinforced Self Compacting Concrete	171
<i>C. Sengul, Y. Akkaya and M.A. Tasdemir</i>	

Determining the Tensile Softening Diagram of Concrete Like Materials using Hybrid Optimisation.....	179
<i>J. Hannawald</i>	
Performance of Plain and Blended Cement Concretes Against Corrosion Cracking..	189
<i>E. Güneyisi, T. Özturan and M. Gesolu</i>	
Mechanical Behavior and Optimum Design of SFRC Plates	199
<i>F. Koksal, A. Ilki, F. Bayramov and M.A. Tasdemir</i>	
Mechanical Properties of Hybrid Fiber Reinforced Concrete	207
<i>A.E. Yurtseven, I.O. Yaman and M. Tokyay</i>	
Influence of Tension Stiffening Effect on Design and Behaviour of Reinforced Concrete Structures	215
<i>A. Elenas, L. Vasiliadis, E. Pouliou and N. Emmanouilidou</i>	
Assessment of Model Parameters for Fracture Simulation in Brittle Disordered Materials like Concrete and Rock	221
<i>J.G.M. van Mier</i>	
Crack Extension due to Corrosion by SiGMA-AE and BEM	233
<i>M. Ohtsu and F.A.K.M. Uddin</i>	
Size Effect on Concrete Splitting Tensile Strength and Modulus of Elasticity	239
<i>A. Kanos, A.E. Giannakopoulos and P.C. Perdikaris</i>	
Mixed-Mode Crack Propagation through Reinforced Concrete	247
<i>J.R. Carmona, G. Ruiz, and J.R. del Viso</i>	

Quantifying Damage for Early Age Concrete

Advanced Analysis of Stresses for Control of Transverse Cracking in Early-Age Concrete Decks of Composite Bridges	259
<i>B.H. Oh and S.C. Choi</i>	
Crack Healing of Early Age Cracks in Concrete	273
<i>E. Schlangen, N. ter Heide and K. van Breugel</i>	
Non-Destructive Monitoring of Fiber Dispersion in FRCS using AC-Impedance Spectroscopy	285
<i>N. Ozyurt, T.O. Mason and S.P. Shah</i>	
Experimental Methodology to Study Plastic Shrinkage Cracks in High Strength Concrete.....	291
<i>A. Sivakumar and M. Santhanam</i>	

Investigation of the Viscoelastic Properties of Fresh Portland Cement Pastes with an Ultrasonic Wave Reflection Method.....	297
<i>Z. Sun and S.P. Shah</i>	
Temperature and Relative Humidity Analysis in Early-age Concrete Decks of Composite Bridges.....	305
<i>B.H. Oh, S.C. Choi and S.W. Cha</i>	
Preliminary Numerical Assessment of Microcracking caused by Autogenous Shrinkage in a Heterogeneous System	317
<i>J.-H. Moon, J. Couch and J. Weiss</i>	
Finite Element Modeling of Early-Age Cracking in Restrained Concrete Ring Specimens	325
<i>O.G. Stavropoulou, M.S. Konsta-Gdoutos and G.E. Papakaliatakis</i>	
Chemical Shrinkage and Calcium Hydroxide Content of Early Age Portland Cement Monitored with Ultrasonic Shear Wave Reflections	331
<i>T. Voigt and S.P. Shah</i>	
 <i>Development of Innovative Cementitious Materials</i>	
A Comparison of HBC & MHC Massive Concretes for Three Gorges Project in China.....	341
<i>T. Sui, J. Li, X. Peng, W. Li, Z. Wen, J. Wang and L. Fan</i>	
Influence of Fly Ash on the Properties of Magnesium Oxychloride Cement.....	347
<i>J. Chan and Z. Li</i>	
Carbonated Cementitious Materials and Their Role in CO ₂ Sequestration.....	353
<i>Y. Shao and S. Monkman</i>	
Mortar Based on Alkali-Activated Blast Furnace Slag.....	361
<i>D. Krizan and M. Komljenovic</i>	
Influence of Temperature and Chemistry Activated on the Cementing Properties of Coal Gangue	367
<i>W. Zhang, S. Zhou, J. Ye, D. Li, and Y. Chen</i>	
Performance Criteria for the Use of FGD Gypsum in Cement and Concrete Production.....	373
<i>G. Tzouvalas, G. Rantis and S. Tsimas</i>	
Cement-Based Nanopiezo 0–3 Composites.....	379
<i>Z. Li and H. Gong</i>	

Concrete Strength Prediction in Structural Elements Made with Pulverised Fuel Ash	385
<i>A. Hatzitheodorou and M.N. Soutsos,</i>	
Study on Properties of Rubber Included Concrete under Wet-Dry Cycling	395
<i>Y. Zhang, Sun Wei and Chen Shengxia</i>	
Reactive Silica of Fly Ash as an Indicator for the Mechanical Performance of Blended Cements.....	403
<i>S.K. Antiohos and S. Tsimas</i>	
Optimization of Ladle Furnace Slag for Use as a Supplementary Cementing Material.....	411
<i>I. Papayianni and E. Anastasiou</i>	
Criteria for the Use of Steel Slag Aggregates in Concrete.....	419
<i>E. Anastasiou and I. Papayianni</i>	

Designing Concrete for Unconventional Properties

Concrete for the Construction Industry of Tomorrow	429
<i>M. Corradi</i>	
Modelling the Influence of SRA on Properties of HPC.....	441
<i>V. López and A. Pacios</i>	
A study of the Interaction Between Viscosity Modifying Agent and High Range Water Reducer in Self Compacting Concrete	449
<i>N. Prakash and M. Santhanam</i>	
Early Hydration of Clinker Phases Analyzed by Soft X-Ray Transmission Microscopy: Effects of Viscosity Modifying Agents.....	455
<i>D.A. Silva and P.J.M. Monteiro</i>	
Rheological Properties and Segregation Resistance of SCC Prepared by Portland Cement and Fly Ash	463
<i>M.H. Ozkul and U.A. Dogan</i>	
Optimization of Superplasticizer Content in Self-Compacting Concrete.....	469
<i>K.A. Melo and W.L. Repette</i>	
Capillary Rheology of Extruded Cement-Based Materials.....	479
<i>K.G. Kuder and S.P. Shah</i>	
Design of High Strength Self-Compacting Concrete For Tunnel Linings	485
<i>B. Barragán, R. Gettu, X. Pintado and M. Bravo</i>	

Quantitative Image Analysis for Microstructural Characterization of Concrete

Characterising the Pore Structure of Cement-Based Materials Using Backscattered Electron and Confocal Microscopy	495
<i>H.S. Wong, M.K. Head and N.R. Buenfeld</i>	
Fractography of Fiber-Cement Composites via Laser Scanning Confocal Microscopy	503
<i>B.J. Mohr and K.E. Kurtis</i>	
Quantification of Capillary Pores and Hadley Grains in Cement Paste Using FIB-Nanotomography.....	509
<i>L. Holzer, P. Gasser and B. Muench</i>	
Three Dimensional Analysis of Air Void Systems in Concrete.....	517
<i>E.N. Landis and D.J. Corr</i>	

Concrete Deterioration, Repair and Rehabilitation

Calculation of Structural Degradation due to Corrosion of Reinforcements.....	527
<i>J. Rodriguez, L. Ortega, D. Izquierdo and C. Andrade</i>	
Archaeological Museums of Rethymnon and Herakleion: Pilot Diagnostic Studies of Corrosion of Steel Reinforcement in Concrete	537
<i>G. Batis, A. Moropoulou, M. Chronopoulos, Ch. Mavronikolas, A. Athanasiadou, A. Bakolas, P. Moundoulas and E. Aggelakopoulou</i>	
Efficiency of Traditional and Innovative Protection Methods Against Corrosion	545
<i>F. Tittarelli and G. Moriconi</i>	
Corrosion of Steel in Cracked Concrete: Experimental Investigation	557
<i>M. Bi and K. Subramaniam</i>	
Criteria and Methodology for Diagnosis of Corrosion of Steel Reinforcements in Restored Monuments	563
<i>A. Moropoulou, G. Batis, M. Chronopoulos, A. Bakolas, P. Moundoulas, E. Aggelakopoulou, E. Rakanta, K. Lambropoulos and E. Daflou</i>	
Using the Chloride Migration Rate to Predict the Chloride Penetration Resistance of Concrete.....	575
<i>S.W. Cho and S.C. Chiang</i>	
Pore-Size Distribution in Blended Cement Pastes Using NMR Techniques	583
<i>M. Katsioti, M.S. Katsiotis, M. Fardis, G. Papavassiliou and J. Marinos</i>	

Investigation of CKD – BFS in Reinforcement Corrosion Protection.....	591
<i>A. Routoulas, S. Kalogeropoulou, P. Pantazopoulou and P. Koulouris</i>	
Strain Monitoring Method Using in Freeze-thaw Test of RC.....	597
<i>H. Pengfei</i>	
Evaluation of Organic Corrosion Inhibitor Effectiveness into Concrete	605
<i>E. Rakanta, E. Daflou and G. Batis</i>	
Using Chloride Concentration and Electrical Current to Determine the Non-Steady-State Chloride Diffusivity from Migration Test.....	613
<i>C.C. Yang and S.C. Chiang</i>	
Concrete Repair According to the New European Standard.....	619
<i>F. Dehn</i>	
Retrofit of Concrete Members with Externally Bonded Prefabricated SFRCC Jackets	625
<i>A. Ilki, D. Akgun, O. Goray, C. Demir and N. Kumbasar</i>	
Internal Stress and Cracking in Stone and Masonry	633
<i>G.W. Scherer</i>	
The Contribution of Historic Mortars on the Earthquake Resistance of Byzantine Monuments	643
<i>A. Moropoulou, K. Labropoulos, P. Moundoulas and A. Bakolas</i>	
Moisture and Ion Transport in Layered Plaster/Substrate Combinations: an NMR Study	653
<i>L. Pel, J. Petkovi and H. Huinink</i>	
Freezing of Salt Solutions in Small Pores.....	661
<i>M. Steiger</i>	
Effect of the Pore Size Distribution on Crystallization Pressure	669
<i>G. Chanvillard and G.W. Scherer</i>	
Optimization Assessment of Compatible Repair Byzantine Concrete for the Historic Structures' Restoration Intervention.....	675
<i>E. Aggelakopoulou, A. Moropoulou and A. Bakolas</i>	
Evaluating the Potential Damage to Stones from Wetting and Drying Cycles.....	685
<i>I. Jiménez González and G.W. Scherer</i>	
Assessment of Atmospheric Pollution Impact on the Microstructure of Marble Surfaces	695
<i>A. Moropoulou, E.T. Delegou, E. Karaviti and V. Vlahakis</i>	

Controlling Stress from Swelling Clay	703
<i>T.P. Wangler, A.K. Wylykanowitz and G.W. Scherer</i>	
<i>FRPs and Textiles in Cement Composites</i>	
Tension Stiffening in GFRP Reinforced Concrete Beams	711
<i>R. Al-Sunna, K. Pilakoutas, P. Waldron and T. Al-Hadeed</i>	
Curved Non Ferrous Reinforcement for Concrete Structures	719
<i>M. Guadagnini, T. Imjai and K. Pilakoutas</i>	
Failure and Instability Analysis of FRP-Concrete Shear Debonding using Stochastic Approach.....	729
<i>K. Subramaniam, M. Ali-Ahmad and M. Ghosn</i>	
Bond Characteristics and Structural Behavior of Inorganic Polymer FRP	735
<i>Ch. Papakonstantinou and P. Balaguru</i>	
Effect of Concrete Composition on FRP/Concrete Bond Capacity	743
<i>J. Pan and C.K.Y. Leung</i>	
Mechanical Properties of Hybrid Fabrics in Pultruded Composites	749
<i>A. Peled, B. Mobasher and S. Sueki</i>	
Improving the Bond Characteristics of a Strand Embedded in a Cementitious Matrix.....	763
<i>B.-G. Kang, B. Banholzer and W. Brameshuber</i>	
Aspects of Modeling Textile Reinforced Concrete (TRC) in 2D	769
<i>J. Hegger and O. Bruckermann</i>	
TRC-Specimens Modeled as a Chain of Cracks Bridged by Bundles	777
<i>R. Chudoba, M. Vorechovsky, J. Jerabek and M. Konrad</i>	
Author Index	785

Preface
of ECF16 Chairman
Emmanuel E. Gdoutos

The "16th European Conference of Fracture," (ECF16), was held in the beautiful town of Alexandroupolis, Greece, site of the Democritus University of Thrace, July 3-7, 2006. Within the context of ECF16 forty six special symposia and sessions were organized by renowned experts from around the world. The present volume is devoted to the symposium on "Measuring, Monitoring and Modeling Concrete Properties" (MMMCP) organized by my wife Dr. Maria Konsta-Gdoutos in honor of our good friend Surendra P. Shah of Northwestern University, USA. I am greatly indebted to Maria for undertaking the difficult task to organize this symposium with great success and edit the symposium volume.

Started in 1976, the European Conference of Fracture (ECF) takes place every two years in a European country. Its scope is to promote world-wide cooperation among scientists and engineers concerned with fracture and fatigue of solids. ECF16 was under the auspices of the European Structural Integrity Society (ESIS) and was sponsored by the American Society of Testing and Materials, the British Society for Stain Measurement, the Society of Experimental Mechanics, the Italian Society for Experimental Mechanics and the Japanese Society of Mechanical Engineers. ECF16 focused in all aspects of structural integrity with the objective of improving the safety and performance of engineering structures, components, systems and their associated materials. Emphasis was given to the failure of nanostructured materials and nanostructures and micro- and nanoelectromechanical systems (MEMS and NEMS). The technical program of ECF16 was the product of hard work and dedication of the members of the Scientific Advisory Board, the pillars of ECF16, to whom I am greatly indebted. As chairman of ECF16 I am honored to have them on the Board and work closely with them for the success of ECF16.

ECF16 has been attended by more than nine hundred participants, while more than eight hundred papers have been presented, far more than any other previous ECF over a thirty year period. I am happy and proud to have welcomed in Alexandroupolis well-known experts, colleague, friends, old and new acquaintances who came from around the world to discuss problems related to the analysis and prevention of failure in structures. The tranquility and peacefulness of the small town of Alexandroupolis provided an ideal environment for a group of scientists and engineers to gather and interact on a personal basis.

I wish to thank very sincerely the editor Dr. Maria Konsta-Gdoutos for the excellent appearance of this volume and the authors for their valuable contributions. Finally, a special word of thanks goes to Mrs. Nathalie Jacobs of Springer who accepted my proposal to publish this special volume and her kind and continuous collaboration and support.

January 2006
Xanthi, Greece

Emmanuel E. Gdoutos
ECF16 Chairman

Editor's Preface

This volume contains 94 papers presented at the symposium on "Measuring, Monitoring and Modeling Concrete Properties," (MMCP), which was organized in honor of Surendra P. Shah, Walter P. Murphy Professor of Northwestern University. The symposium took place under the umbrella of the 16th European Conference of Fracture in Alexandroupolis, Greece, on July 3-7, 2006. The book is dedicated to Surendra P. Shah, a researcher, teacher, and advocate for the cement and concrete sciences, in recognition of his continuous, original, diversified and outstanding contributions for half a century.

The book consists of invited papers written by leading experts in the field. It contains original contributions concerning the latest trends and developments in measuring, modeling, and monitoring concrete properties. Fourteen keynote papers were contributed by B.L. Karihaloo, H. Stang, M. Corradi, G.W. Scherer, K. Pilakoutas, M.A. Tasdemir, J. van Mier, F. Dehn, D. Cusson, T. Sui, B.H. Oh, B. Mobasher, N.R. Buenfeld and C. Andrade.

The papers cover a wide range of subjects including fracture and mechanisms of deterioration of cementitious composites, engineering performance and modeling for early-age, high-performance fiber-reinforced cementitious composites and development of innovative cementitious materials. They are arranged in the following 8 sections:

The first section on *engineering performance and modeling for high-performance cementitious composites (HPFRCs)*, contains nineteen papers dealing with computational and experimental micro-mechanical modeling of the mechanical behaviour of HPFRCs and the micro-structural modeling of their durability characteristics.

The second section on *fracture and deformation of cement based composites* contains eleven papers dealing with a mechanical behavior and fracture of conventional and new cement based composites, advanced methods for crack detection in concrete, obtaining three-dimensional information of fracture processes, and new developments on the fracture toughness of concrete including high strength concrete and size effects.

The third section on *quantifying damage for early age concrete* contains nine papers dealing with realistic assessment and modeling for mechanical behavior of early age concrete, autogenous shrinkage and microcracking in heterogeneous systems.

The fourth section on *development of innovative cementitious materials* contains twelve papers dealing with performance criteria on the incorporation of industrial byproducts in concrete and cementitious composites.

The fifth section on *designing concrete for unconventional properties* contains eight papers dealing with the use of chemical admixtures such as superplasticizers, shrinkage

reducing admixtures and viscosity modifying agents for designing the composition of concretes with special rheological properties, such as self compacting concrete.

The sixth section on *quantitative image analysis for microstructural characterization of concrete* contains four papers dealing with the use of imaging technology as a basis to quantify and model the variability in the nano-, micro-, and meso-structure of concrete.

The seventh section on *concrete deterioration, repair and rehabilitation* contains twenty two papers dealing with new concepts for the processing of repair and rehabilitation measures of concrete structures, the development of predicting models characterizing the corrosion process of steel in concrete and a special session on the deterioration of historic building materials and the development of crystallization pressure and the initiation and propagation of cracks from growth of salt crystals.

Finally, the eighth section on *FRPs and textiles in cement composites* contains nine papers dealing with the bond characteristics and structural behaviour of new reinforcing materials such as fiber reinforced plastics and hybrid fabrics, and the modeling of textile reinforced concrete.

I consider it an honor and privilege I have had the opportunity to edit this volume. I wish to thank very sincerely the authors who have contributed to this volume and all those who participated in the symposium on "Measuring, Monitoring and Modeling Concrete Properties" to honor Surendra P. Shah, a great friend and a colleague, whose work will be indelibly imprinted on the pages of cement and concrete science history.

All those involved in the work of this symposium are gratefully acknowledged, in particular Professor E.E. Gdoutos for organizing ECF16 from start to finish and the members of the Scientific Committee for soliciting and reviewing of papers. Finally, a special word of thanks goes to Ms Nathalie Jacobs of Springer for her interest in publishing this work and her kind collaboration and support.

March, 2006
Xanthi, Greece

Maria S. Konsta-Gdoutos
Editor

Surendra P. Shah

***Walter P. Murphy Professor
Northwestern University, Evanston, Illinois, USA***

Professor Surendra P. Shah's career began as most of ours begin. Shah, who grew up in India, began his academic career there where he received his undergraduate degree from B.V.M. College. His graduate work began at Lehigh University where he completed his Masters of Science. He then took two years to work as a design engineer at Modjeski and Masters. During this time he met and married Dorothie Crispell. Suru then attended Cornell University, where he received his Ph.D. in civil engineering under the advisement of Professors George Winter, Richard White, and Floyd Slater. After receiving his Ph.D. he was ready to begin the journey that would establish him as a leading figure in the research and teaching in the field of cement and concrete sciences.

In 1965, Suru joined the faculty of the Materials Engineering Department at the University of Illinois at Chicago (UIC). There he taught courses in civil engineering and materials science while developing a state-of-the-art research laboratory. In 1981, he joined the faculty of Northwestern University where he is now a Walter P. Murphy Professor. His research continues to focus on synthesizing materials science, mechanics and structural engineering by combining our knowledge of different scales. He pioneered research to better understand and develop new materials. He has written over 400 journal articles, co-edited 20 symposium proceedings, co-authored two textbooks, and served as the editor-in-chief for the journal, *Materials and Structures*. His foresight in research led to the establishment of the National Science Foundation Center for Science and Technology of Advanced Cement-Based Materials (ACBM). His leadership at ACBM has provided the opportunities for growth of research in the field, as well as the growth of cement-based curriculum in undergraduate programs around the world. As he built a strong research base, he was developing the next wave of researchers and educators.

Suru Shah has been a strong advocate in the training of future scientists in the cement and concrete field. Through his work at ACBM, he established a network of faculty whose goal is to increase the amount of time spent teaching cement sciences as well as improving the tools for teaching. Through the establishment of the Undergraduate Faculty Workshop, ACBM has reached over 100 faculty and in turn, influenced over 10,000 students. This is not to say that Suru has not influenced his fair share of students on his own. During his tenures at UIC and Northwestern, he has advised over 160 graduate students and 80 post-doctoral fellows. His influence in these student's academic careers has been recognized at both UIC and Northwestern as the recipient of Excellence in Teach-

ing awards. Suru's strong commitment to teaching is evident by the number of his students who have joined the ranks of academia. As a result of the enduring partnership of ACBM with industry, many of his students are enjoying successful careers in the industrial sector.

Surendra Shah's dedication to the field is evidenced by the innovations he has brought about through his research and teaching. Acknowledgement of this work is further established by his recent election to the National Academy of Engineering, the most prestigious award given in the engineering field. Over his career, he has received many other awards including the ACI Phiello Award, the Swedish Concrete Award, the RILEM Gold Medal, the ASCE-CERF Charles Pankow Award, and the ASTM Thompson Award. ACI, RILEM and the University of Dundee have organized symposia in his honor. In addition to his work in cement and concrete sciences, Suru is a strong proponent of the arts. He is an avid stage fan, including opera, theatre, and the symphony. He is a movie buff and, it is no secret that, he is a wine and food aficionado. Surendra P. Shah epitomizes the phrase "Renaissance Man."

Suru Shah is a man who has pushed the envelope in all areas of cement and concrete technology and in doing so, has inspired professionals, researchers, and, students to do the same. He has no immediate plans for retirement. He will continue his mission as a teacher, researcher, and advocate for the cement and concrete sciences. It is with a deep sense of honor and respect that this book and symposium are dedicated to the work and legacy of Surendra P. Shah.

March, 2006
Xanthi, Greece

Maria S. Konsta-Gdoutos
Editor

SCIENTIFIC ADVISORY BOARD

Professor G. Batis,
NTUA, Greece

Professor T. N. Bittencourt,
University of Sao Paolo, Brazil,

Dr. D. Corr,
Northwestern University, USA

Professor R. Faria,
University of Porto, Portugal

Dr. F. Dehn,
*Institute for Materials Research and Testing
(Germany)*

Professor R. Gettu,
Indian Institute of Technology, India

Professor B. Karihaloo,
Cardiff University, UK

Professor K.E. Kurtis,
Georgia Institute of Technology, USA

Professor Z. Li,
HKUST, Hong Kong

Dr. C.K.Y. Leung,
HKUST, Hong Kong

Professor B. Mobasher,
Arizona State University, USA

Professor A. Moropoulou,
NTUA, Greece

Professor B.H. Oh,
Seoul National University, Korea

Professor I. Papayianni,
Aristotle University of Thessaloniki, Greece

Professor P.C. Perdikaris,,
University of Thessaly, Greece

Dr. A. Peled,
Ben Gurion University, Israel

Professor K. Pilakoutas,
The University of Sheffield, UK

Dr. W. L. Repette,
UFSC, Brazil

Professor G. W. Scherer,
Princeton University, USA

Professor H. Stang,
Technical University of Denmark, Denmark

Dr. K. Subramaniam,
*City College of the City University of New
York, USA*

Professor M.A. Tasdemir,
Istanbul Technical University, Turkey

Professor J.G.M. Van Mier,
ETH Zurich, Switzerland

Dr. J. Weiss,
Purdue University, USA

***Engineering Performance and
Modeling for High-Performance
Cementitious Composites***

EFFECT OF FIBRE DISTRIBUTION ON THE FATIGUE PERFORMANCE AND AUTOGENOUS SHRINKAGE OF CARDIFRC[®]

D. Nicolaides, A. Kanellopoulos and B.L. Karihaloo
*School of Engineering, Cardiff University, Queen's Buildings, P.O. Box 925,
Cardiff CF24 0YF, UK*

Abstract: This paper describes a recent fatigue performance check on the high performance fibre-reinforced cementitious composite CARDIFRC[®]. It is shown that an even distribution of fibres throughout the bulk of the material is crucial to its excellent fatigue performance. Moreover, the even distribution of fibres is also a key factor in the reduction of the autogenous shrinkage strains in this material. The aim of this investigation is to reveal the reason behind the low fatigue life and large scatter in the autogenous shrinkage strains of CARDIFRC, when large test specimens were used. It is confirmed to be due to poor distribution of fibres in the large specimens.

Key Words: Fatigue, shrinkage, fibre distribution

1. INTRODUCTION

The mechanical performance of any HPRC depends to a high degree on the even distribution of fibres in the bulk of the material. Any regions with a low concentration of fibres or with no fibres are potential sites of weakness. The distribution of fibres in the mix depends on several factors, e.g. on how the fibres were introduced into the mix, on the vibration frequency during compaction, and on the size and shape of the object cast from CARDIFRC. The distribution of fibres within the matrix of the beam is a critical parameter affecting the fatigue performance of steel fibre reinforced concrete. It is, however, extremely difficult to achieve an even distribution of fibres in large specimens. Failure to attain this goal may result in an extremely low fatigue life, whereas a proper and even fibre distribution can guarantee an extremely long fatigue life. This is more evident in the case of HPRCs, where the interfacial bond between the fibres and the matrix is particularly strong, due to the dense structure of the material. The difficulty in achieving an even distribution of fibres is more pronounced in thicker specimens (e.g. 100 mm),

whereas the even distribution can be achieved without difficulty in specimens with a relatively small thickness (e.g. 35 mm). The uneven fibre distribution in the matrix also affects measurement of autogenous shrinkage in large specimens of CARDIFRC®.

2. FATIGUE EXPERIMENTAL PROCEDURE

Specimens of Dimensions 100x100x500 mm

Fatigue tests were carried out in three-point bending in a stiff self-straining testing frame fitted with a DARTEC 2500 kN dynamic-static actuator on 100x100x500 mm beams made of CARDIFRC® mix I. The beams were simply supported over a span of 400 mm. Four short cylindrical clamps were set on the supports to prevent the beam from moving, during the cyclic load application. These clamps did not actually come in contact with the specimen, unless it started moving from its original position. The machine was powered by a 23 lit/min DARTEC hydraulic pump and was connected with a DARTEC 9600 Digital Feedback Controller. Four types of measurement were recorded for each beam: (1) the load from the load cell of the testing machine; (2) the vertical deflection at the mid-span; (3) the time from the start of load application; and (4) the number of cycles to failure.

The vertical mid-span deflection was measured by a single LVDT. This LVDT was calibrated for a very narrow range of deformation (± 2.5 mm), because the deformation of the beam during its fatigue life was expected to be very small. In this way, it was also anticipated to minimise the noise in this particular measurement. A mechanical stop was installed 10 mm below the centre of the beam in order to prevent damage to the LVDT if the beam suddenly failed. All the data were acquired using DT800 dataTaker logger and stored temporarily in its memory before they were downloaded to the connected computer. The DT800 dataTaker is a data acquisition and logging instrument, which has the ability to operate in burst mode. In this mode, DT800 can sample at very high rates, but only for short periods of time. This mode of operation is appropriate for fatigue data acquisition and logging. The logging procedure was controlled by appropriate software, called DeLogger Plus. This software package contains a powerful set of tools for working with DT800, like the programme builder option. This option allows the user to define the number and types of the scan channels, the time interval to trigger each scan, the quantity to be read (e.g. voltage) and how to convert the reading into appropriate engineering units.

Fatigue tests are generally carried out for a given constant minimum stress or for a constant ratio between the minimum and maximum stress levels. In this study, a constant minimum stress level of 10% of the static flexural strength was maintained. The cyclic tests were carried out at maximum stress levels ranging from 70% to 85% of the monotonic strength. The fatigue tests were performed in load control. The ultimate static load in three-point bending equalled $P_u = 57$ kN. This value resulted if the standard deviation of the peak load measured in static three point bend tests was subtracted from the mean value. Each specimen was first subjected to three slow cycles between 2 kN and 28 kN, which corresponded to a stress level of 50% of the monotonic strength. It should be noted that specimens tested in this study were not pre-cracked before cyclic loading, so the selected stress level of 50% lies within the elastic range of the material response. This is an essential characteristic of this study compared with previous studies on fatigue of fibre

reinforced concrete. The specimens were preloaded for stabilisation purposes. The test stopped automatically after the specimen failure or after one million cycles, whichever occurred first.

The specimens were subjected to a sinusoidal cyclic loading with a frequency of 6 Hz. The choice of the frequency was dictated by the time required for the test beam to reach 1000000 cycles and by the need to avoid undesirable side effects because of high frequencies. Despite the fact that several researchers have conducted fatigue tests with frequencies up to 20 Hz, these values were considered too high to maintain an accurate load range and to minimise the effects of inertia. On the other hand, frequencies of 1-2 Hz were considered too low to complete a full test (up to 1000000 cycles) within a reasonable time period. Therefore, a frequency of 6 Hz was selected and a full test was completed in less than 48 hours.

3. RESULTS AND DISCUSSION

Tests have been performed in the load ranges between 10%-85%, 10%-80% and 10%-70% of the ultimate flexural strength. Table 1 and Figure 1 show the fatigue life of specimens 100x100x500 mm (i.e. number of cycles to failure, N). It is clear that there is a large scatter in the experimental fatigue life, which is a characteristic of the fatigue tests. This is attributed to the nature of the material and also to errors in test variables, which are repeated in a large number of cycles. The large scatter in the experimental results did not give an opportunity to discern a trend in the fatigue life of the material, not even after a large number of tests were performed.

The large scatter in the fatigue life of the tested beams is mainly attributed to the inhomogeneous nature of the material. The addition of fibres to the concrete matrix can dramatically improve the fatigue performance of the composite and also impart it with additional strength in tension, shear and flexure. It is, however, extremely difficult to achieve an even distribution of fibres within the mix, because of the large quantity of fibres used. This has the effect that some internal vertical planes of the specimen under flexure will be devoid of fibres. In the worst case that the planes devoid of fibres are located in the region of the maximum bending moment, they become the failure planes after only very few cycles. Another important consideration is the orientation of the fibres in the region of the maximum bending moment.

The failure surfaces of the tested beams were thoroughly examined visually. It was observed that beams that failed after a very small number of cycles, had large areas in these planes almost devoid of fibres, especially in the zones of tensile stress. Others had a significant number of fibres in these planes, but these were oriented vertically, i.e. they did not exert any closure pressure across the plane of failure. On the other hand, specimens that withstood a large number of cycles before failure, had an even distribution of fibres crossing the plane of failure, and most of them applied substantial closure pressure, thus extending the fatigue life of the beams. In the case of the beams that withstood 1000000 cycles without failure, the planes of failure (revealed after the specimens were broken) were full of fibres (most of them long), all of them exerting closure pressure. It can be concluded that the distribution of fibres within the matrix of the beam is a very important parameter affecting the fatigue life of the tested specimens.

Table 1. Number of cycles sustained by cardifrc - mix i beams (100x100x500 mm)

Fatigue Tests - CARDIFRC [®] - Mix I Beams (100x100x500 mm)			
Beam Number	10% - 85% Pu	10% - 80% Pu	10% - 70% Pu
1	706	9918	5910
2	181738	2144	18
3	18	14	437
4	2510	4036	1000000
5	41539	28733	279
6	169279	911453	4
7	1000000	195703	1000000
8	6174	9337	3
9	4918	131237	527988
10	161839	78940	110999
11	493	-	-
12	54977	-	-

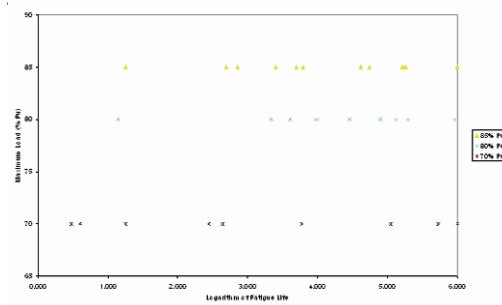


Figure 1. Fatigue life of CARDIFRC - Mix I beams (100x100x500 mm)

It is, however, extremely difficult to achieve an even distribution of fibres in the mix. For the improvement of fibre distribution, the fibres are added to the mix through vibrating sieves; for 6 mm long fibres, a 5 mm sieve is used and for 13 mm long fibres a 12 mm sieve is used. Many interesting observations regarding the fibre distribution in CARDIFRC were made by the image analysis of specimens, which will be discussed later.

There was a suspicion that the poor distribution of the fibres within the specimen was also a result of the high frequency of compaction 100 Hz (on an electric vibrating table) used during the casting of the specimens as a result of which the fibres were forced to the sides of the beams. In order to confirm or dispel this suspicion, some of the remaining 100x100x500 mm specimens were cut into six smaller specimens of dimensions 33x100x250 mm, as shown in Figure 2.

The cut specimens were tested statically in three-point bending under displacement control, and the peak loads were noted. The average peak loads for top, middle and bottom specimens were:

Top Specimens: $P_{u,top} = 4.30$ kN

Middle Specimens: $P_{u,mid} = 6.09$ kN

Bottom Specimens: $P_{u,bot} = 11.31$ kN

It can be clearly observed that the ultimate load from the flexural static tests is much lower at the top, and is significantly increased when moving to middle and finally bottom specimens. The bottom specimens give the highest value of peak load, which is a clear indication that these specimens had more fibres, in comparison with the top and middle specimens. These experimental results undoubtedly confirm the suspicion of the poor distribution of fibres within the original specimens, as a result of the high frequency of almost 100 Hz used during the compaction of the cast specimens.

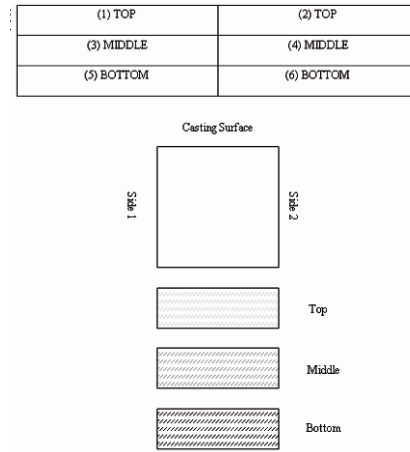


Figure 2. Schematic presentation of the cut specimens and the fibre density in the top, middle and bottom specimens

Specimens of Dimensions 35x90x360 mm

After the completion of the static tests on the cut specimens, where it was clearly revealed that the high vibration frequency had produced poor distribution of the fibres, it was decided to cast smaller CARDIFRC[®], Mix I beams, 360x90x35 mm, and use a frequency during compaction not exceeding 50 Hz. The selected dimensions were regarded to be more realistic, in the sense that CARDIFRC[®] is a material that is mainly intended for use for repairing and strengthening in thin strips of about 20 mm thickness.

For the fatigue tests, it was decided to use a value of ultimate load equal to $P_u = 10$ kN. This value is two standard deviations less than the mean value of the peak load obtained earlier from static three-point bend experiments, i.e. $P_u = P_{avg} - 2S.D.$ The subtraction of two standard deviations from the average peak load increases the probability that the ultimate monotonic load of all specimens tested in fatigue would be lower than

the applied P_u , to about 95.5%. This choice was aimed at minimising the factors that caused the huge scatter in fatigue life of the 100x100x500 mm beams, and eventually at obtaining more consistent results.

The fatigue tests were carried out in three-point bending, in the same way as was described earlier for the 100x100x500 mm beams. The tests were performed under load control between two limits (with a sinusoidal force variation in time). The minimum stress level, S_{min} , was 10% of the monotonic strength and the maximum stress level, S_{max} , ranged from 80% to 90% of the monotonic strength. Before the cyclic loading was applied, the beams were preloaded with 3 static loading/unloading cycles between 1 kN and 5 kN, the higher load corresponding to 50% of the monotonic flexural strength of the material. The specimens were preloaded for stabilisation purposes. The frequency of loading used was 6 Hz. The tests stopped after specimen failure or after one million cycles, whichever occurred first. In the special case of two specimens, it was decided to test them up to a larger number of cycles.

Tests have been performed in the load ranges between 10%-80%, 10%-85% and 10%-90% of the ultimate flexural strength. Table 2 gives the fatigue life of specimens (i.e. number of cycles to failure, N). It is immediately noticeable that there is an excellent consistency in the fatigue life for the load ranges between 10%-80% and 10%-85%, since all of the eight specimens sustained 1000000 or more cycles without failure. This is attributed to the smaller thickness of these specimens (35 mm), the lower frequency used during the vibration of these specimens, which ensures a more even distribution of the fibres within the specimens, and also to the choice of P_u as equal to $P_{avg}-2SD$, as explained above.

Table 2. Flexural fatigue tests experimental results (CARDIFRC[®] - MIX I, 360x90x35 mm)

Load Amplitude (% P_u)	Fatigue Life (N)				Average Fatigue Life (N)
	N_1	N_2	N_3	N_4	
10-90%	1000000	21564	9315	1000000	-
10-85%	1000000	1000000	1000000	20000000	1000000 ^(*1)
10-80%	1000000	1000000	1000000	2000000	1000000 ^(*1)

*1 The average fatigue life considers only the first 1000000 cycles sustained by specimen No.4.

An important observation from the tests performed at maximum load levels of 80% and 85% P_u , is the fact that none of the eight tested specimens developed any visible cracks during the 1000000 cycles, attesting once again to the improved distribution of the fibres within these specimens. It also implies that probably no specimen will fail at lower maximum stress levels. From the above experimental results, it can be concluded that the endurance limit of the material is approximately at 85% of its flexural strength. Below this limit none of the tested specimens failed, not even after a very large number of cycles (e.g. 20000000 cycles). Slightly above this load limit, some specimens did not fail after 1000000 cycles, whereas some others failed after a relatively small number of cycles. Another remark about the observed fatigue limit is that it is very high, not very often observed in the relevant literature. This is an indication that CARDIFRC[®] has an extensive elastic zone. This is confirmed by direct tension tests performed by Benson (2003).

In order to check whether internal cracks had developed in the specimens that sustained 1000000 or more cycles without failure, they were tested afterwards in static three-point bending. The purpose of this static testing was to compare the post-fatigue flexural strengths and static envelope curves with the pre-fatigue test results. None of the specimens had any visible external cracks at the end of fatigue testing. The specimens tested at 80%, 85% and 90% P_u in fatigue, showed a small increase in their flexural strength (Table 3). This increase seemed to be higher than could be attributed to the increase due to age alone. It is believed to depend on the maximum flexural fatigue stress (S_{max}) to which the specimens were subjected earlier. From the available evidence, it was anticipated that with lower S_{max} values the increase in flexural strength would be higher. This was however not confirmed experimentally, since the increase of the flexural strength for specimens tested earlier up to 80%, 85% and 90% P_u was of the same order of magnitude. A remarkable observation was that the specimens which did not fail after 1000000 cycles up to 90% P_u , showed the highest increase (7%), whereas the lowest increase (5%) was observed for specimens tested earlier up to 80% P_u . The increase observed in specimens tested earlier up to 85% P_u was about 6%.

Although it seems that there exists a linear correlation between the fatigue loading stress and the corresponding post-fatigue static flexural strength, no definite conclusions can be drawn. The difference is believed to be very small; therefore the increase in the flexural strength is assumed to be of the same order of magnitude for the three groups. Moreover, the result of the average strength for specimens tested up to 90% P_u , was based only on two specimen results, which did not fail after fatigue. It is believed that the increase in flexural strength is approximately constant for specimens subjected to fatigue stress close to the fatigue limit of the material. This result confirms previously noted results in the literature, that prior cycling may lead to an improvement in strength (Naaman and Hammoud, 1998; Ramakrishnan et al., 1996; Naaman and Harajli, 1990). It has been suggested that this increase in strength is due to densification of the material, caused by stress cycling. It is also known that most FRCs are linearly elastic up to about 80% or more of the matrix tensile strength and that the microcracking process starts beyond this point. This leads to the conclusion that beam specimens subjected to cyclic flexural stress below this level are not likely to have a reduced first crack flexural strength (Ramakrishnan and Lokvik, 1992). However, the mechanisms behind the increase of the post-fatigue flexural strength in HPRCCs are still unclear.

Table 3. Experimental peak loads and tensile/flexural strengths of CARDIFRC® - MIX I beams (360x90x35 mm), tested in 3 – point bending, after they have been subjected first to fatigue loading

Beam Number	10%-90% Pu		10%-85% Pu		10%-80% Pu	
	P_u (kN)	f_t (MPa)	P_u (kN)	f_t (MPa)	P_u (kN)	f_t (MPa)
1	14.65	55.81	12.65	48.19	14.30	54.48
2	-	-	14.64	55.77	13.70	52.19
3	-	-	14.30	54.48	12.40	47.24
4	12.88	49.07	13.33	50.78	13.60	51.81
Average Strength		52.44		52.30		51.43

4. IMAGE ANALYSIS OF FATIGUE SPECIMENS

Due to the large scatter observed in the fatigue life of large CARDIFRC[®] - Mix I beams (100x100x500 mm), it was decided to investigate the fibre distribution in the planes of failure of six specimens tested under fatigue loading (between 10-70% P_U). The fatigue life of the selected specimens varied between a very small number of cycles (less than a decade) and a very high number of cycles (more than 500000 cycles). In addition, the distribution of fibres in a section of a specimen that did not fail after 1000000 cycles was also investigated. This particular specimen was cut along a predetermined section, located in the centre of the beam, using a diamond saw. In the case of specimens that failed under fatigue loading, the planes of failure had to be flattened first before examination under the microscope. This was also done using a diamond saw, as close as possible to the actual plane of failure. The exact number of cycles sustained by each of the selected specimens and the average number of fibres (/cm²) resulting from the image analysis of their planes of failure are shown in Table 4. Other statistical measures are given in Table 5.

Table 4. Average number of fibres resulting from image analysis of specimens tested under fatigue loading

No. of Cycles	Average No. of Fibres (/cm ²)	Max. No. of Fibres (/cm ²)	Notes
3	120	Theoretical result based on the solution of “ <i>the Buffon needle problem</i> ”. For a 10x10x10 mm cube, the total number of fibres in a cut section, equals $\underline{215/cm^2}$.	All specimens (100x100x500 mm) made of CARDIFRC [®] - Mix I and tested in fatigue between 10-70% P_U .
4	116		
437	125		
5910	131		
110999	159		
527988	174		
>1000000	194		

The conclusion from this investigation is that a high average number of fibres in the plane of failure is a guarantee for an extended fatigue life of the specimen. The case of the specimen that sustained just 4 cycles is an exception, since the average number of fibres is lower than the specimen that sustained 3 cycles. It is, however, important to note that both specimens have an average number of fibres lower than that in the specimens that sustained higher number of cycles. All planes of failure examined have at least one grid where the maximum counted number of fibres is equal or very close to the theoretical maximum resulting from the solution of the “*Buffon needle problem*” (Nicolaidis, 2004). On the other hand, the minimum fibre count varies significantly between the selected specimens. This discrepancy is reflected clearly in the values of standard deviation and coefficients of variation. It is apparent that the decreased standard deviation, which means a more even distribution of fibres within the matrix, leads to a higher number of cycles to failure. The same conclusion is also supported by the coefficients of variation, which also decrease as the fatigue life increases.

Table 5. Statistical analysis of the results of the image analysis of specimens tested under fatigue loading

No. of Cycles	Average No. of Fibres (/cm ²)	Max. Count	Min. Count	Standard Deviation (SD)	Coefficient of Variation (COV) (%)
3	120	215	5	70.30	61
4	116	215	5	66.02	55
437	125	215	28	58.89	47
5910	131	202	27	37.73	29
110999	159	212	72	28.32	18
527988	174	213	127	20.82	12
>1000000	194	215	138	14.54	7

Specimens that sustained a very small number of cycles (3 and 4 cycles) have a very heterogeneous distribution of fibres in their planes of failure. It is clear from Figures 3-5 that large areas of these sections have a significantly lower density of fibres. The areas with lower density of fibres are located in both cases in the bottom of the specimens. This is very important, since these parts of the beams were subjected to tension, and a lower number of fibres made it easy for a crack to initiate, resulting in extremely low fatigue life. Although the upper parts of these sections have a higher number of fibres, this was not sufficient to prevent their fast fracture. It must be mentioned that at some locations in the examined sections the number of counted fibres was extremely small, less than ten (Table 5). The average number of fibres in these two sections was 118 (/cm²).

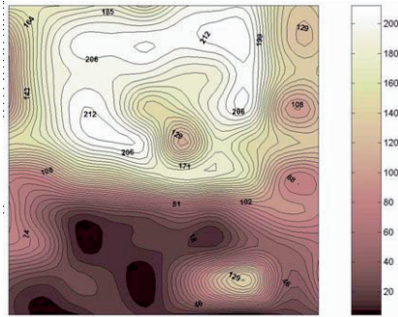


Figure 3. Contour plot showing the fibre distribution for the 100x100 mm beam plane of failure, after fatigue testing between 10-70% P_u (failure after 4 cycles)

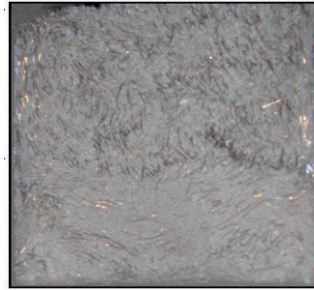


Figure 4. Plane of failure of the 100x100 mm beam after fatigue testing between 10-70% P_u (failure after 4 cycles)

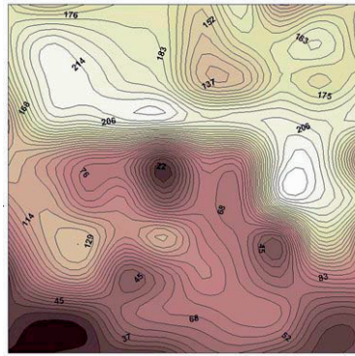


Figure 5. Contour plot showing the fibre distribution for the 100x100 mm beam plane of failure, after fatigue testing between 10-70% P_u (failure after 3 cycles)

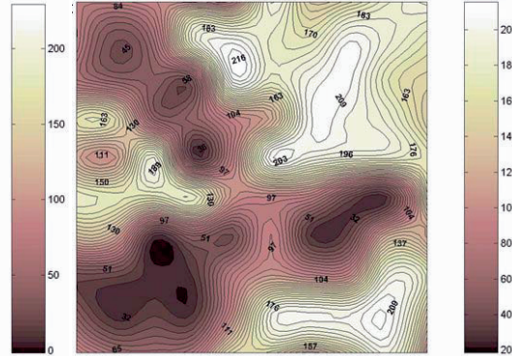


Figure 6. Contour plot showing the fibre distribution for the 100x100 mm beam plane of failure, after fatigue testing between 10-70% P_u (failure after 437 cycles)

The third specimen under examination that sustained a slightly higher number of cycles (437 cycles) also had a heterogeneous distribution of fibres in the plane of failure. It is very apparent that three main regions, covering a large fraction of the total section, have a considerably lower density of fibres, as shown in Figure 6. The average number of fibres in this section is 125 (/cm²), which is higher than the number of fibres counted in the sections of specimens that sustained lower number of cycles.

The fourth specimen under investigation, which failed after 5910 cycles, had a generally uniform distribution of fibres in the plane of failure, apart from an area at the bottom of the beam and extending up to the centre, where the fibre concentration was noticeably lower (Figure 7). The average number of fibres in this section is 131 (/cm²), which is higher than the number of fibres counted in the sections of specimens that sustained lower number of cycles.

Specimens that sustained significantly higher number of cycles (110999 and 527988), have a considerably higher number of fibres in their planes of failure (159/cm² and 174/cm², respectively) (Figures 8, 9). The distribution of fibres is also generally even, with the exception of some areas with lower fibre concentration. It is believed that these areas facilitated the crack initiation and propagation within these sections.

Finally, in the case of the specimen that did not fail after the application of 1000000 cycles, the even distribution of fibres is very noticeable, which in combination with the significantly higher average number of fibres (194/cm²), satisfactorily explains why the specimen did not fail during testing (Figure 10).

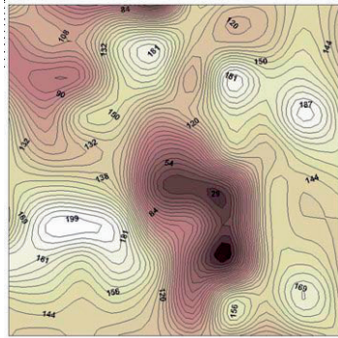


Figure 7. Contour plot showing the fibre distribution for the 100x100 mm beam plane of failure, after fatigue testing between 10-70% P_u (failure after 5910 cycles)

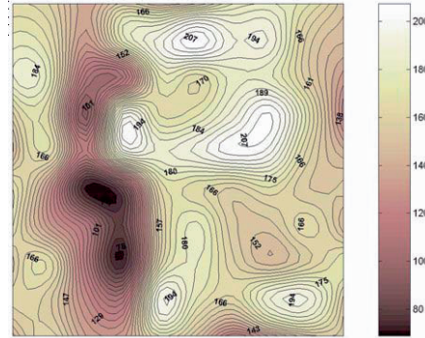


Figure 8. Contour plot showing the fibre distribution for the 100x100mm beam plane of failure, after fatigue testing between 10-70% P_u (failure after 110999 cycles)

Considering that the theoretical maximum number of fibres per cm^2 resulting from the solution of the “*Buffon needle problem*” (Nicolaidis, 2004) is 215, it can be concluded that the closer the number of fibres in the plane of failure is to the theoretical maximum, the higher the number of cycles it will sustain (Figure 11). This result is very important in the light of an existing correlation between the image analysis and CT-scanning analysis, as shown by Nicolaidis (2004). By applying the non-destructive CT imaging method, the maps of the X-ray absorption density of the specimen can be produced. The magnitude of the X-ray absorption in several areas of the section can lead to an estimate of the corresponding numbers of fibres in those areas (based on the correlation between X-ray absorption density and corresponding number of fibres), and therefore to an estimation of the expected fatigue life of the specimen.

5. AUTOGENOUS SHRINKAGE

Autogenous shrinkage experiments conducted on large (100x100x500 mm) CARDIFRC[®] members revealed a large scatter in the measured strains as a consequence of the uneven distribution of fibres into the matrix, as shown in the Figures 3-10. This large scatter is clearly seen from the entries in Table 6 and Figure 12. The spread of the results is very large, since even at the end of the first 10 hours the COV is relatively high for such set of data. These tests were therefore discontinued after 90 hours. Smaller specimens with the same dimensions as those used for fatigue testing were used for measuring autogenous shrinkage strains. These specimens gave very consistent results with very low scatter.